Improving the performance of inorganic-organic hybrid photovoltaic devices by uniform ordering of ZnO nanorods and near-atmospheric pressure nitrogen plasma treatment

Seungjun Oh, Takahiro Nagata, János Volk, and Yutaka Wakayama

Citation: J. Appl. Phys. **113**, 083708 (2013); doi: 10.1063/1.4793283
View online: http://dx.doi.org/10.1063/1.4793283
View Table of Contents: http://jap.aip.org/resource/1/JAPIAU/v113/i8
Published by the American Institute of Physics.

JOURNAL OF APPLIED PHYSICS **113**, 083708 (2013)

Improving the performance of inorganic-organic hybrid photovoltaic devices by uniform ordering of ZnO nanorods and near-atmospheric pressure nitrogen plasma treatment

Seungjun Oh,[1,2] Takahiro Nagata,[1] János Volk,[3] and Yutaka Wakayama[1,2,a)]
[1]*International Center for Materials Nanoarchitectonics (WPI-MANA), National Institute for Materials Science, 1-1 Namiki, Tsukuba 305-0044, Japan*
[2]*Department of Chemistry and Biochemistry, Faculty of Engineering, Kyushu University, 1-1 Namiki, Tsukuba 305-0044, Japan*
[3]*Research Centre for Natural Sciences, Hungarian Academy of Sciences, 1025 Budapest, Pusztaszeri út 59-67, Hungary*

(Received 16 November 2012; accepted 8 February 2013; published online 26 February 2013)

We investigated the performance of hybrid photovoltaic devices composed of ZnO and poly (3-hexylthiophene) (P3HT). The uniform ordering of ZnO nanorods (NRs) and nitrogen plasma treatment at near-atmospheric pressure offer advantages in modifying the ZnO NR surface. Uniform ordering of the ZnO NRs promoted the effective infiltration of P3HT, increasing the donor–acceptor interface area, which is directly related to short-circuit current density (J_{SC}). Near-atmospheric pressure treatment compensated carriers to form a highly resistant interlayer at the ZnO surface, which reduced carrier recombination and, as a result, increased the open circuit voltage (V_{OC}). Combining these two approaches achieved five-fold increase in J_{SC} compared to that of the planar heterojunction, while the V_{OC} was increased up to 0.71 V. © *2013 American Institute of Physics*. [http://dx.doi.org/10.1063/1.4793283]

I. INTRODUCTION

In recent years, extensive studies of hybrid photovoltaic (HPV) devices, composed of organic light-harvesting conjugated polymers and inorganic semiconductors, have increased interest in renewable energy.[1–8] HPV devices promise advantages of both organic and inorganic materials. Organic materials offer high light absorption coefficients, flexibility, ease of processing, and structural diversity. Inorganic materials offer mechanical hardness and thermal stability, as well as various electronic properties ranging from those of insulator to semiconductor to metallic conductor.

The creation of HPV devices faces two major challenges. One is how to obtain a high density of inorganic nanorods (NRs) so as to increase the donor–acceptor interface area, which is directly related to the short-circuit current density (J_{SC}).[9,10] Such NRs are also expected to provide direct pathways to the electrodes after exciton dissociation. Although there have been many efforts to obtain a high density of inorganic NRs,[1,3,5,11,12] the random orientation of the NRs prevents infiltration of the light-absorbing polymer into the NR array. For example, J_{SC} could reach ~2.5 mA/cm^2 if the whole surface of ZnO NRs 60 nm in diameter and 600 nm tall contributed to the interface, but only half of the ideal J_{SC} was reached.[3] In addition, the random orientation limits the controllability of the diameter, spacing, and height of the NRs.[13] NRs should be strictly perpendicular to the substrate surface, and the dimensions should be uniform, to increase the donor–acceptor interface area.

The other major challenge for the creation of high-efficiency HPV devices is how to improve the open circuit voltage (V_{OC}). In a simple approximation, V_{OC} depends on the energy level difference between the conduction band minimum of the inorganic acceptor and the highest occupied molecular orbital of the polymer donor. In HPV devices based on conjugated poly(3-hexylthiophene) (P3HT) and ZnO, for example, the V_{OC} estimated from work functions using the electron affinity rule is 1.6 V.[14,15] However, the V_{OC} measured in actual devices is around 0.4 ± 0.1 V less owing to recombination losses.[1–3,8,9] One possible reason is that the surface of the ZnO has a very narrow depletion region where separated photocarriers (electrons and holes) are very close to each other, allowing their recombination.[16] Another reason is that dark carriers diffuse from the cathode owing to the high electron mobility of ZnO,[17–20] causing recombination losses between the photocarriers and the dark carriers.[21] Several approaches to reducing these recombination losses have been investigated by introducing interfacial surface dipoles,[22] alkanethiol self-assembled monolayers,[23] and insulating layers such as Al_2O_3 and CdS as recombination barriers.[24,25] Although interlayers like Al_2O_3 and CdS at the ZnO–P3HT interface improve V_{OC}, they can generate unfavorable interfacial trap states. Furthermore, additional depositions of these interlayers disturb the precise control of the dimensions and surface morphology of ZnO NRs. A potential alternative is nitridation. Free electrons in the ZnO can be compensated by the substitution of oxygen vacancies with nitrogen atoms. Such a compensated ZnO surface layer would be insulating and would work as a recombination barrier without any dimensional or morphological change. Additionally, plasma treatments make possible a large area and homogeneous nitrogen passivation even on patterned indented oxide surfaces.[26] However, conventional plasma treatments create defects in the oxides, which can act as

a)E-mail address: WAKAYAMA.Yutaka@nims.go.jp. Tel.: +81 29 860 4403. Fax: +81 29 860 4916.

carrier trap sites. To resolve this, we used a nitrogen plasma treatment in which the discharge pressure was kept at near-atmospheric pressure (NAP). Such high-pressure plasma produces high-density active nitrogen species and allows effective plasma treatment even at room temperature. As a result, nitride passivation can be achieved with fewer defects.

Here, we applied two approaches for two major challenges described above. First, we demonstrate how uniformly ordered ZnO NRs increase J_{SC}. Second, NAP treatment was performed on the surface of ZnO NRs in order to increase V_{OC}. We investigated the electronic structures of the NAP-treated ZnO surface by a combination of X-ray photoelectron spectra and dark current–voltage measurement to prove the effectiveness of NAP treatment at improving V_{OC}.

II. EXPERIMENTAL DETAILS

A. Sample fabrication

Figure 1 illustrates the basic setup of the sample configuration. Details of the growth process of the ordered ZnO NR array on a transparent conductive (TCO) layer are described in our previous paper.[13] First, ZnO/Al-doped ZnO (AZO)/ZnO multilayers were prepared on c-sapphire substrates by a pulsed laser deposition technique using a KrF excimer laser (248 nm). The first ZnO film on the sapphire substrate is needed as a buffer for the following epitaxial growth of the AZO film. The AZO layer acted as a TCO layer and controlled NR growth. The sheet resistance of the transparent AZO film was confirmed to be 600 Ω/sq with a four-point contact probe method (Napson, Model RG-80 N); the AZO film can be used as an electrode for solar cells in the same way as a conventional indium tin oxide (ITO) substrate. The top ZnO layer acts as a "seed layer" to initiate the following ZnO NR growth. The substrate temperatures were optimized for epitaxial growth of the respective layers. The buffer layer was deposited in two steps: First, a 200-nm layer was deposited at a substrate temperature of 500 °C, and then a 50-nm layer was deposited at 580 °C. Then, a 200-nm AZO film and a 200-nm ZnO seed layer were deposited at 300 °C.

Before the ZnO NRs were grown, the initial nucleation sites were patterned by nanoimprint lithography.[13] Polymethylmethacrylate (PMMA) films with a thickness of 100 nm were spin-coated onto the substrate as resist layers. A mold with an array of square pillars 100 nm wide, high, and apart was used for patterning. The area of the pillar array was 1 cm × 1 cm. The mold was pressed onto the PMMA resist layer at 135 °C and 10 MPa for 10 min. The surface was then dry etched with oxygen plasma gas to remove all residual PMMA resist. The ZnO NRs were grown in a sealed glass container filled with an aqueous solution of zinc nitrate hexahydrate ($Zn(NO_3)_2{\cdot}6H_2O$) and hexamethylenetetramine ($C_6H_{12}N_4$) with an equimolar concentration of 0.012M at 85 °C for 6 h.[27,28] Finally, the PMMA resist was removed in acetone and ethanol, and the NRs were immediately rinsed with deionized water.

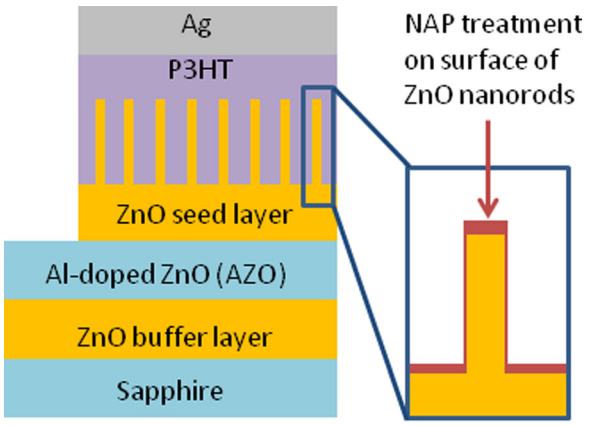

FIG. 1. Schematic illustration of device configuration.

The surface of the NRs was treated with nitrogen plasma at room temperature for 30 min. The flow of N_2 (99.9999%) was fixed at 400 sccm by a mass flow controller. The discharge pressure was kept at 40 kPa (NAP). Nitrogen plasma was generated by applying alternating pulsed voltages of 7 kV at 30 kHz between two parallel-plate electrodes with a uniform gap of 1 mm.

P3HT solution (5 wt. % in chlorobenzene) was spin-coated onto both untreated (UT-) and nitrogen plasma–treated (NAP-) ZnO NRs. P3HT films were also formed on a flat ZnO substrate (planar P3HT/ZnO) and on randomly oriented ZnO NRs without NAP treatment for comparison. The randomly oriented ZnO NRs were prepared on a polycrystalline ITO substrate with a 200-nm-thick ZnO seed layer.[13] All samples were annealed at 180 °C in a vacuum ($\sim 1 \times 10^{-2}$ Pa) to enhance the infiltration of P3HT between the ZnO NRs. Finally, 100-nm Ag electrodes were deposited on top of the multi-layers in vacuum ($\sim 1 \times 10^{-5}$ Pa).

B. Sample characterization

The alignment of the ZnO NRs was observed by scanning electron microscope (SEM; SU8000; Hitachi). The chemical bonding states of the surfaces of UT- and NAP-ZnO NRs were evaluated by X-ray photoelectron spectroscopy (XPS; Theta Probe; Thermo) using a monochromated Al Kα X-ray at an energy of 1486.6 eV.[29] The samples were connected to the electrical ground of the system by conductive copper tapes during the XPS measurements. The work function of the system was calibrated with reference to the Au $4f_{7/2}$ and Ag $3d_{5/2}$ peak positions. The total energy resolution was set at 700 meV. Measured binding energies were referenced to the adventitious carbon peak at 285.0 eV. Dark current–voltage was measured at room temperature with a semiconductor parameter analyzer (B1500A; Agilent). The photovoltaic performances of these samples were evaluated under AM1.5 G solar radiation at 100 mW/cm^2.

III. RESULTS AND DISCUSSION

A. Improvement in short-circuit current (J_{SC})

The AZO film was grown on a sapphire substrate to obtain a flat, single-crystal seed layer, which was critical in growing highly oriented epitaxial ZnO NRs.[13] The top-view SEM images of the thus-prepared ZnO NRs show well-aligned, uniform ZnO NRs in the 1 cm × 1 cm area of the

mold (Fig. 2(a)). The NRs measured 120 nm wide and 80 nm apart. A tilted SEM image shown in the inset in Fig. 2(a) confirms a uniform height of about 500 nm. In contrast, the rough surface of the ITO substrates caused random orientations of the ZnO NRs (Fig. 2(b)) in spite of the assistance of the lithographically predefined PMMA resist. These results can be attributed to the roughness and polycrystallinity of the ITO layer.[30,31]

Figure 3 shows the photovoltaic performances of the P3HT/ZnO HPV device. The photovoltaic performance of the planar heterojunction on the AZO substrate was measured as a reference. Both the V_{OC} and the J_{SC} of the planar heterojunction were in good agreement with previous reports.[3,32] The V_{OC} of all samples was almost constant, at $\sim 0.34 \pm 0.04$ V. In contrast, variation in the J_{SC} was clear. This variation should be proportional to the P3HT/ZnO interface area. In the case of ideally ordered ZnO NRs, the interface area is 7.5 times that of the planar heterojunction, which is estimated from the unit cell as depicted in the inset of Fig. 3. In contrast, the J_{SC} of the P3HT/randomly oriented ZnO NRs was only twice that of the planar heterojunction. There are three possible reasons for the disturbance in the increase in J_{SC}. First, the P3HT did not infiltrate completely into the randomly oriented ZnO NR array,[33,34] thus decreasing the actual interfacial area. Second, the random orientation of the ZnO NRs limits their density.[13] Third, the random NRs include abnormally long NRs, which can cause leakage of the photo-current to the anode. Thus, the randomly oriented ZnO NRs are limited in their ability to increase the J_{SC}. On the other hand, the J_{SC} of the P3HT/uniformly ordered ZnO NRs was 5 times that of the planar heterojunction. Such a large increase in J_{SC} can be attributed to the increased interface area. The uniform ordering of the ZnO NRs permits smooth infiltration of the P3HT, increasing the donor–acceptor interface area. However, the J_{SC} did not reach the ideal value. Although most of the ZnO NRs were the same height, some longer NRs also grew (not shown here).[13] We suppose that damage to the surface of the seed layer during the imprinting and dry etching processes triggered the longer NR growth. Thus, J_{SC} could be further improved by further optimization of the patterning and etching conditions, as well as by refined resolution of the nanoimprint lithography.[35]

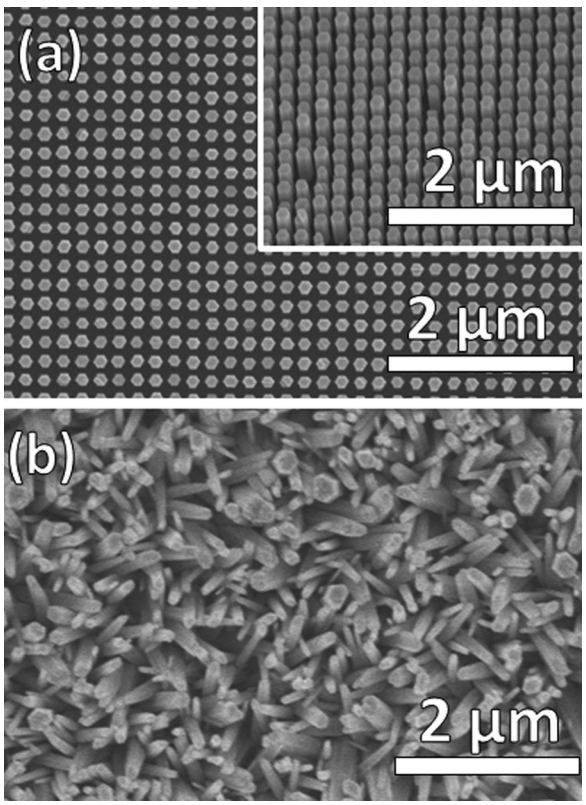

FIG. 2. SEM images of ZnO NRs grown in a predefined pattern on (a) AZO and (b) ITO substrates. The height of the ZnO NRs on the AZO substrate was highly uniform, as shown in a 30°-tilted SEM image (inset in (a)).

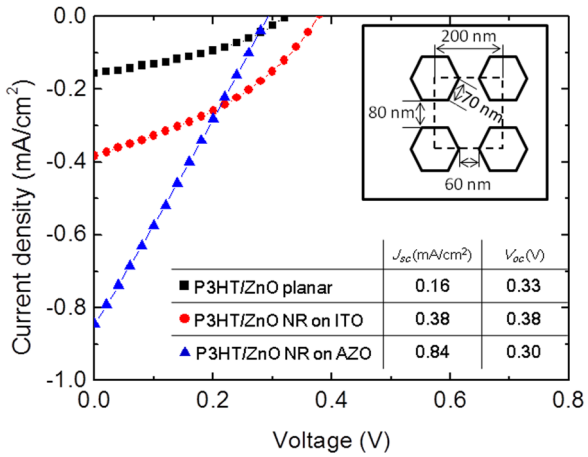

FIG. 3. Photovoltaic performances of the P3HT/uniformly ordered ZnO NRs on (▲) AZO substrate and (●) P3HT/randomly orientated ZnO NRs on ITO substrate. (■) Performance of planar heterojunction as reference. Inset shows the dimensions of the uniformly ordered ZnO NRs. The table summarizes the performances (J_{sc} and V_{oc}) of each device.

B. Improvement in open circuit voltage (V_{OC})

We showed the effect of the uniformly ordered ZnO NRs on the increase in J_{SC} in Sec. III A. The purpose of this section is to increase in the open circuit voltage (V_{OC}). For this purpose, NAP treatment was performed on the surface of uniformly ordered ZnO NRs.

First, we examined the impact of the NAP treatment on the surface morphology of ZnO NRs. Figures 4(a) and 4(b) show SEM images of the ZnO NRs before and after NAP treatments, respectively. As shown here, we confirmed that the NAP treatment induced no change in the surface morphology. For more detailed analyses, we investigated the surface electronic structures of the uniformly ordered UT- and NAP-ZnO NRs by XPS. Four peaks around 396, 398, 400, and 404 eV were detected in an N 1*s* core-level XPS spectrum of the NAP-ZnO NRs (Fig. 5(a)). Both peaks at 396 and 398 eV were assigned to the N–Zn bonding states formed between substitutional N atoms in O-sites (N_O) and neighboring Zn atoms.[36–41] The small peak around 400 eV originated from N–H or C–N species.[39–41] The peak at 404 eV can be assigned to N_2 molecules occupying the position on the oxygen sites ($(N_2)_O$).[36,38,40,41] Both N_O and $(N_2)_O$ can reduce the oxygen vacancies, which act as donors to dope electrons in ZnO.[42] Theoretical calculation predicts

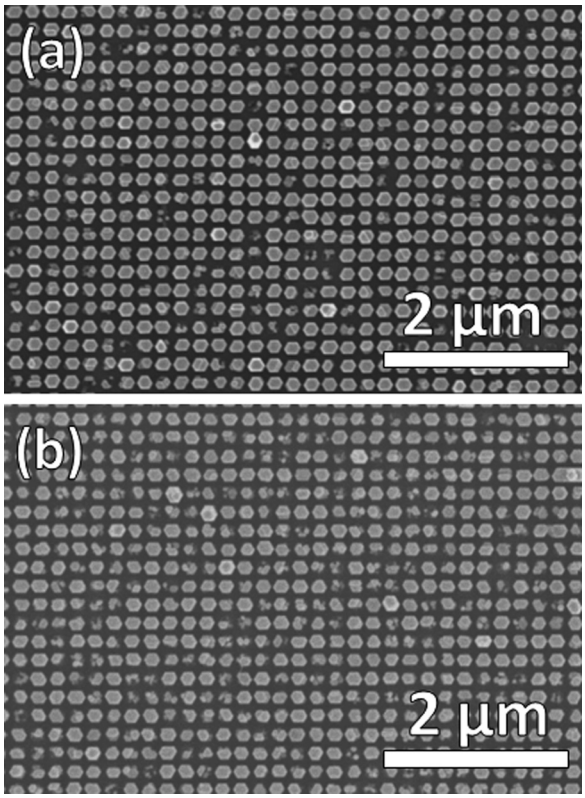

FIG. 4. SEM images of the ZnO NRs (a) before and (b) after NAP treatments. There was no change in the morphology of ZnO NRs before and after NAP treatments.

that N_O works as an acceptor and that $(N_2)_O$ works as a shallow double donor.[43] Judging from the larger signal from N_O than from $(N_2)_O$, we expect NAP treatment to provide acceptors to compensate intrinsic electrons in ZnO.

To confirm the carrier compensation in the ZnO, we examined the variation in the Fermi level of the ZnO by XPS measurements in the valence band regions. The valence band spectra of both the UT- and NAP-ZnO NRs were dominated by the O 2*p*-derived valence band. Here, the valence band maximum (VBM) with respect to the Fermi level is defined by extrapolating the leading edge of the O 2*p*-derived valence band to its intersection with background counts near the Fermi level (arrows in the inset of Fig. 5(b)). The VBM of the NAP-ZnO NRs was slightly shifted toward lower binding energy than that of the UT-ZnO NRs (by 0.3 ± 0.1 eV). There are two potential reasons for this shift: carrier compensation, which causes a shift in the Fermi level to the mid-gap; and a change in the band structure due to Zn–N bondings.

We investigated the core spectra of Zn and O to figure out these issues. The Zn $2p_{3/2}$ peak at 1021.6 eV (solid line in Fig. 5(c)) verified the Zn–O bonding state in the UT-ZnO NRs.[44] After the NAP treatment, the Zn $2p_{3/2}$ peak became asymmetrical, for one of two possible reasons: upward band bending due to the variation in the Fermi level at the surface; and an additional chemical bond formation of Zn–N (1021.1 eV).[45] However, weak intensity of the N 1*s* signal (Fig. 5(a)) shows that the contribution of Zn–N bonding is negligible. Hence, the origin of the peak shift can be attributed mostly to the Fermi level shift to the mid-gap of ZnO. NAP treatment induced two recognizable variations in the O 1*s* spectra: a peak shift toward lower energy and an increase in a shoulder around 531.5 eV (Fig. 5(d)). The peak at 530 eV represents O–Zn bonding states,[46] the shift of which is consistent with the Fermi level shift. The shoulder peak fraction around 531.5 eV was increased after the NAP treatment; that is, the shoulder peak consisted mainly of O–N bonds around 531.2 eV, although O–H or O_2 adsorbed on the surface can also contribute.[36,41,47] These results of the core spectra of Zn and O clarified that the NAP treatment has no

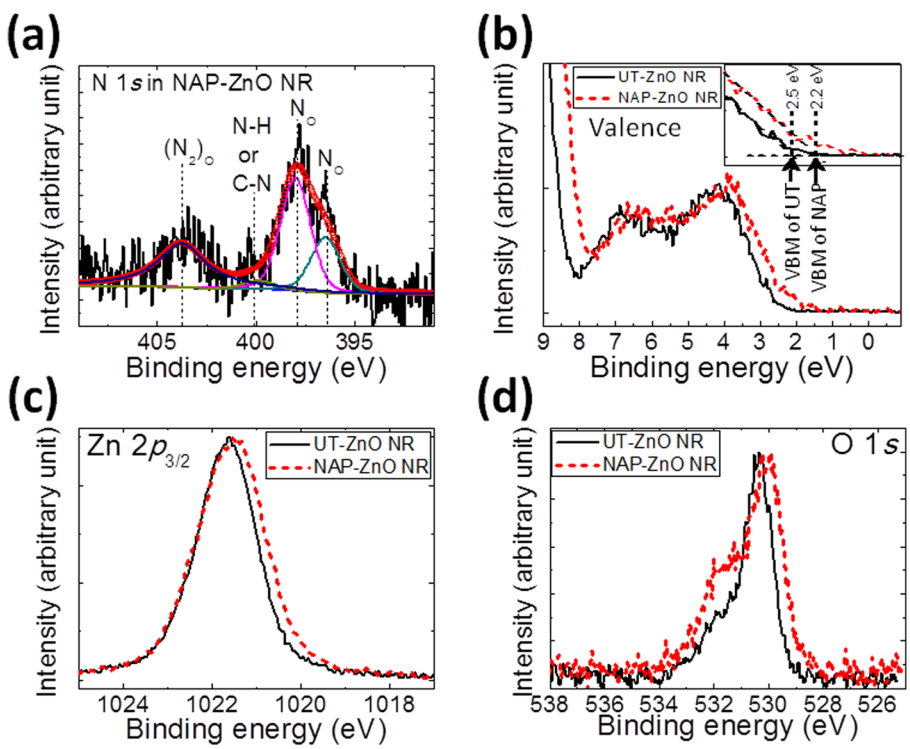

FIG. 5. XPS spectra of (a) N 1*s* core level in NAP-ZnO NRs and of (b) valence band regions, (c) Zn $2p_{3/2}$ core level, and (d) O 1*s* core level in (—) UT-ZnO NRs and (- - -) NAP-ZnO NRs.

influence on the band structure of ZnO. Therefore, we conclude that the Fermi level moved to the mid-gap as a result of carrier compensation.

Figure 6(a) shows the dark current–voltage characteristics of the P3HT/NAP- and UT-ZnO NR heterojunctions. The P3HT/NAP-ZnO NRs show a clear decrease in the dark current. A possible reason is that the NAP-treated surface offers high resistance, reducing the dark carriers from the electrode. This is consistent with the above discussion based on the XPS measurements: NAP treatment compensates carriers to increase the resistivity at the ZnO surface. A schematic energy-level alignment at the P3HT/ZnO interface in Figure 6(a) shows that the NAP-ZnO interlayer, the Fermi level of which is seated around the mid-gap, is insulating and works as a recombination barrier at the interface of P3HT and ZnO.

Figure 6(b) shows the photovoltaic performances of the samples. The V_{OC} of P3HT/NAP-ZnO NRs increased remarkably up to 0.71 V. The high-resistance interlayer inhibited the injection of dark carriers (electrons) to protect the recombination with the holes in P3HT. Additionally, the interlayer probably enhances the dissociation of photo-generated electron and holes by reducing their recombination.[48] Both effects increase carrier lifetime and, consequently, V_{OC}. On the other hand, the J_{SC} of P3HT/NAP-ZnO NRs was almost comparable to that of P3HT/UT-ZnO NRs. Although a small decrease in the J_{SC} is observed, this can be attributable to the deviation of each sample caused by some defects in the NRs. Therefore, we conclude that the NAP treatment affects mainly on the increase in V_{OC}.

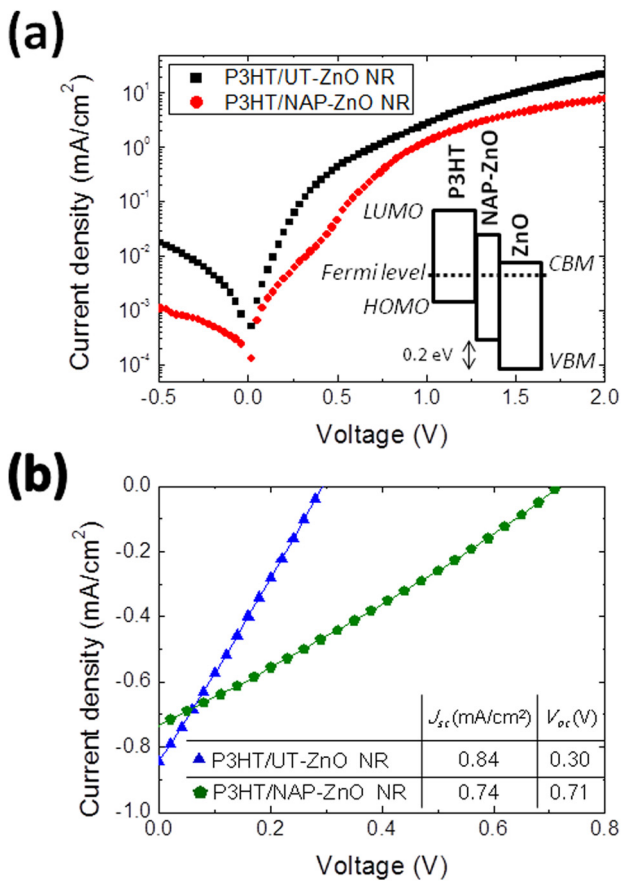

FIG. 6. (a) Dark current–voltage characteristics of (●) P3HT/NAP-ZnO NRs and (■) P3HT/UT-ZnO NRs. Inset shows a schematic energy-level alignment at the P3HT/ZnO interface. (b) Photovoltaic performances of (▲) P3HT/UT-ZnO NR and (■) P3HT/NAP-ZnO NR heterojunctions.

IV. CONCLUSION

We examined two ways to improve the J_{SC} and V_{OC} of HPV devices consisting of P3HT and ZnO NRs. First, uniform ordering of ZnO NRs increased the donor–acceptor interface area, which is directly related to J_{SC}. The J_{SC} was consequently five times that of a planar heterojunction. The uniform ordering of the ZnO NRs thus formed a large donor–acceptor interface area to increase J_{SC}. Second, NAP treatment of the surface of the ZnO NRs improved V_{OC}. Characterization of the electronic structures and dark current measurements revealed that NAP treatment caused a highly resistant layer to form on the ZnO surface. This layer works as a barrier to protect against dark carrier injection and to reduce photo-carrier recombination. As a result, V_{OC} was increased by 0.4 V. Although there is still room for improvement, NAP treatment and the creation of highly ordered ZnO NRs increased V_{OC} and J_{SC}.

ACKNOWLEDGMENTS

This work was supported in part by the Bilateral Joint Project between Hungary and Japan established by the Japan Society for the Promotion of Science (JSPS). Part of this work was performed in the MANA Foundry, which is part of the World Premier International Research Center Initiative (WPI Program) established by the Ministry of Education, Culture, Sports, Science and Technology. J.V. acknowledges the support of the János Bólyai Research Scholarship of the Hungarian Academy of Sciences and the Hungarian Fundamental Research Fund (OTKA PD 77578).

[1]L. Baeten, B. Conings, H.-G. Boyen, J. D'Haen, A. Hardy, M. D'Olieslaeger, J. V. Manca, and M. K. V. Bael, Adv. Mater. **23**, 2802 (2011).
[2]J. J. Uhlrich, R. Franking, R. J. Hamers, and T. F. Kuech, J. Phys. Chem. C **113**, 21147 (2009).
[3]B. Conings, L. Baeten, H.-G. Boyen, D. Spoltore, J. D'Haen, L. Grieten, P. Wagner, M. K. V. Bael, and J. V. Manca, J. Phys. Chem. C **115**, 16695 (2011).
[4]J. J. Uhlrich, D. C. Olson, J. W. P. Hsu, and T. F. Kuech, J. Vac. Sci. Technol. A **27**(2), 328 (2009).
[5]Y. Hao, J. Pei, Y. Wei, Y. Cao, S. Jiao, F. Zhu, J. Li, and D. Xu, J. Phys. Chem. C **114**, 8622 (2010).
[6]S. Wu, Q. Tai, and F. Yan, J. Phys. Chem. C **114**, 6197 (2010).
[7]M. T. Lloyd, Y.-J. Lee, R. J. Davis, E. Fang, R. M. Fleming, and J. W. P. Hsu, J. Phys. Chem. C **113**, 17608 (2009).
[8]A. M. Peiró, P. Ravirajan, K. Govender, D. S. Boyle, P. O'Brien, D. D. C. Bradley, J. Nelson, and J. R. Durranta, J. Mater. Chem. **16**, 2088 (2006).
[9]D. C. Olson, Y.-J. Lee, M. S. White, N. Kopidakis, S. E. Shaheen, D. S. Ginley, J. A. Voigt, and J. W. P. Hsu, J. Phys. Chem. C **111**, 16670 (2007).
[10]F. Yang, M. Shtein, and S. R. Forrest, Nature Mater. **4**, 37 (2005).
[11]J. Qiu, X. Li, F. Zhuge, X. Gan, X. Gao, W. He, S.-J. Park, H.-K. Kim, and Y.-H. Hwang, Nanotechnology **21**, 195602 (2010).
[12]S. Yamabi and H. Imai, J. Mater. Chem. **12**, 3773 (2002).
[13]S. Oh, T. Nagata, J. Volk, and Y. Wakayama, Appl. Phys. Express **5**, 095003 (2012).
[14]M. C. Gwinner, Y. Vaynzof, K. K. Banger, P. K. H. Ho, R. H. Friend, and H. Sirringhaus, Adv. Funct. Mater. **20**, 3457 (2010).

[15]M. Onoda, K. Tada, A. A. Zakhidov, and K. Yoshino, Thin Solid Films **331**, 76 (1998).
[16]T. Nagata, S. Oh, Y. Yamashita, H. Yoshikawa, N. Ikeno, K. Kobayashi, T. Chikyow, and Y. Wakayama, Appl. Phys. Lett. **102**, 043302 (2013).
[17]P. F. Carcia, R. S. McLean, M. H. Reilly, and G. Nunes, Appl. Phys. Lett. **82**, 1117 (2003).
[18]E. M. Kaidashev, M. Lorenz, H. von Wenckstern, A. Rahm, H.-C. Semmelhack, K.-H. Han, G. Benndorf, C. Bundesmann, H. Hochmuth, and M. Grundmann, Appl. Phys. Lett. **82**, 3901 (2003).
[19]T. Makino, Y. Segawa, A. Tsukazaki, A. Ohtomo, and M. Kawasaki, Appl. Phys. Lett. **87**, 022101 (2005).
[20]M. Law, L. E. Greene, J. C. Johnson, R. Saykally, and P. Yang, Nature Mater. **4**, 455 (2005).
[21]Y.-X. Wang, S.-R. Tseng, H.-F. Meng, K.-C. Lee, C.-H. Liu, and S.-F. Horng, Appl. Phys. Lett. **93**, 133501 (2008).
[22]C. Goh, S. R. Scully, and M. D. McGehee, J. Appl. Phys. **101**, 114503 (2007).
[23]T. C. Monson, M. T. Lloyd, D. C. Olson, Y.-J. Lee, and J. W. P. Hsu, Adv. Mater. **20**, 4755 (2008).
[24]L. E. Greene, M. Law, B. D. Yuhas, and P. Yang, J. Phys. Chem. C **111**, 18451 (2007).
[25]E. D. Spoerke, M. T. Lloyd, E. M. McCready, D. C. Olson, Y.-J. Lee, and J. W. P. Hsu, Appl. Phys. Lett. **95**, 213506 (2009).
[26]T. Nagata, M. Haemori, J. Anzai, T. Uehara, and T. Chikyow, Jpn. J. Appl. Phys., Part 1 **48**, 040206 (2009).
[27]J. Volk, T. Nagata, R. Erdélyi, I. Bársony, A. L. Tóth, I. E. Lukács, Zs. Czigány, H. Tomimoto, Y. Shingaya, and T. Chikyow, Nanoscale Res. Lett. **4**, 699 (2009).
[28]R. Erdélyi, T. Nagata, D. J. Rogers, F. H. Teherani, Z. E. Horváth, Z. Lábadi, J. Baji, Y. Wakayama, and J. Volk, Cryst. Growth Des. **11**, 2515 (2011).
[29]T. Nagata, S. Oh, T. Chikyow, and Y. Wakayama, Org. Electron. **12**, 279 (2011).
[30]H. Park, K.-J. Byeon, K.-Y. Yang, J.-Y. Cho, and H. Lee, Nanotechnology **21**, 355304 (2010).
[31]H. Jeong, K. S. Kim, Y. H. Kim, H. Jeong, H. Song, K. H. Lee, M. S. Jeong, D. Wang, and G. Y. Jung, Nanotechnology **22**, 275310 (2011).
[32]J. Boucle, H. J. Snaith, and N. C. Greenham, J. Phys. Chem. C **114**, 3664 (2010).
[33]D. C. Olson, J. Piris, R. T. Collins, S. E. Shaheen, and D. S. Ginley, Thin Solid Films **496**, 26 (2006).
[34]P. Ravirajan, A. M. Peiró, M. K. Nazeeruddin, M. Graetzel, D. D. C. Bradley, J. R. Durrant, and J. Nelson, J. Phys. Chem. B **110**, 7635 (2006).
[35]S. Y. Chou, MRS Bull. **26**(7), 512 (2001).
[36]X. H. Li, H. Y. Xu, X. T. Zhang, Y. C. Liu, J. W. Sun, and Y. M. Lu, Appl. Phys. Lett. **95**, 191903 (2009).
[37]C. L. Perkins, S. H. Lee, X. N. Li, S. E. Asher, and T. J. Coutts, J. Appl. Phys. **97**, 034907 (2005).
[38]J. Z. Wang, E. Elamurugu, V. Sallet, F. Jomard, A. Lusson, A. M. Botelho do Rego, P. Barquinha, G. Gonçalves, R. Martins, and E. Fortunato, Appl. Surf. Sci. **254**, 7178 (2008).
[39]Z. Y. Xiao, Y. C. Liu, J. Y. Zhang, D. X. Zhao, Y. M. Lu, D. Z. Shen, and X. W. Fan, Semicond. Sci. Technol. **20**, 796 (2005).
[40]P. Cao, D. X. Zhao, J. Y. Zhang, D. Z. Shen, Y. M. Lu, B. Yao, B. H. Li, Y. Bai, and X. W. Fan, Appl. Surf. Sci. **254**, 2900 (2008).
[41]J. P. Zhang, L. D. Zhang, L. Q. Zhu, Y. Zhang, M. Liu, X. J. Wang, and G. He, J. Appl. Phys. **102**, 114903 (2007).
[42]Y. Ma, G. T. Du, T. P. Yang, D. L. Qiu, X. Zhang, H. J. Yang, Y. T. Zhang, B. J. Zhao, X. T. Yang, and D. L. Liu, J. Cryst. Growth **255**, 303 (2003).
[43]Y. Yan, S. B. Zhang, and S. T. Pantelides, Phys. Rev. Lett. **86**, 5723 (2001).
[44]B. Vincent Crist and XPS International LLC, *Handbooks of Monochromatic XPS Spectra* (XPS International LLC, USA, 2005), p. 820.
[45]G. Z. Xing, D. D. Wang, B. Yao, L. F. N. Ah Qune, T. Yang, Q. He, J. H. Yang, and L. L. Yang, J. Appl. Phys. **108**, 083710 (2010).
[46]M. Futsuhara, K. Yoshioka, and O. Takai, Thin Solid Films **317**, 322 (1998).
[47]N. Tabet, M. Faiza, and A. Al-Oteibi, J. Electron Spectrosc. Relat. Phenom. **163**, 15 (2008).
[48]B. C. O'Regan, S. Scully, A. C. Mayer, E. Palomares, and J. Durrant, J. Phys. Chem. B **109**, 4616 (2005).